Comparison of Heterologously Expressed Human Cardiac and Skeletal Muscle Sodium Channels

Dao W. Wang, Alfred L. George, Jr., and Paul B. Bennett
Departments of Pharmacology and Medicine, Vanderbilt University School of Medicine, Nashville, Tennessee 37232-6602 USA

ABSTRACT In this study we have expressed and characterized recombinant cardiac and skeletal muscle sodium channel α subunits in tsA-201 cells under identical experimental conditions. Unlike the *Xenopus* oocyte expression system, in tsA-201 cells (transformed human embryonic kidney) both channels seem to gate rapidly, as in native tissue. In general, hSkM1 gating seemed faster than hH1 both in terms of rate of inactivation and rate of recovery from inactivation as well as time to peak current. The midpoint of the steady-state inactivation curve was ~25 mV more negative for hH1 compared with hSkM1. In both isoforms, the steady-state channel availability relationships ("inactivation curves") shifted toward more negative membrane potentials with time. The cardiac isoform showed a minimal shift in the activation curve as a function of time after whole-cell dialysis, whereas hSkM1 showed a continued and marked negative shift in the activation voltage dependence of channel gating. This observation suggests that the mechanism underlying the shift in inactivation voltage dependence may be similar to the one that is causing the shift in the activation voltage dependence in hSkM1 but that this is uncoupled in the cardiac isoform. These results demonstrate the utility and limitations of measuring cardiac and skeletal muscle recombinant Na^+ channels in tsA-201 cells. This baseline characterization will be useful for future investigations on channel mutants and pharmacology.

INTRODUCTION

Voltage-gated sodium channels are the molecular basis for the rapid influx of sodium that occurs in most excitable tissues during the upstroke of the action potential. This forms the electrical basis for neuronal conduction as well as for excitation-contraction coupling in skeletal muscle and in heart (Armstrong, 1981). Sodium channels from rat brain (Noda et al., 1986a,b), heart (Rogart et al., 1989; Gellens et al., 1992), and skeletal muscle (Trimmer et al., 1989; George et al., 1992) exhibit a high degree of amino acid similarity. Nevertheless, they are derived from unique genes and are immunologically and pharmacologically distinct (see Catterall, 1992). One striking distinction among these channels are their different sensitivities to tetrodotoxin and saxitoxin. Brain and skeletal muscle channels are blocked by nanomolar concentrations, whereas micromolar concentrations are required to block the cardiac isoform (see Hille, 1992).

Other functional similarities and distinctions among these channels are less clear. Apparent differences in gating can be deduced from the literature, yet studies are often carried out in various preparations and under different experimental conditions (Aldrich et al., 1983; Yue and Marban, 1989; Valenzuela and Bennett, 1994). Are these distinctions due to differences in protein structure or in experimental conditions? The goal of this study was to express the recombinant cardiac and skeletal muscle sodium channel α subunits in mammalian cells under identical conditions. It is important to investigate the molecular and biophysical nature of the human Na^+ channels; however, it is difficult to obtain human tissue for study. For these reasons, the availability of channels in a cultured cell model system is important. Cardiac Na^+ channels are targets of antiarrhythmic drugs whose action depends on channel gating. Thus, it is necessary to understand whether these distinct proteins are truly functionally distinct. These experiments form the basis for future studies using the Na^+ channel isoform-specific amino acid differences to probe potential functional differences by site-directed mutagenesis and generation of chimeric sodium channels.

MATERIALS AND METHODS

Voltage-clamp methods

Macroscopic sodium currents from cells transfected with either hH1 or hSkM1 were recorded using the whole-cell method of the patch-clamp technique. When filled with the intracellular solution, electrodes had resistances ranging from 0.8 to 2 MΩ, with an average of 1.47 MΩ ± 0.06 MΩ (n = 87). Voltage-clamp command pulses were generated by microcomputer using pCLAMP software (v6.0 Axon Instruments, Foster City, CA). Recorded membrane currents were filtered at 5 kHz (−3dB, 4-pole Bessel filter). An Axopatch 200 patch-clamp amplifier was used with series resistance compensation. Data were analyzed using pCLAMP software and our own custom programs. The standard holding potential for all pulse protocols was −120 mV. Data are presented as mean ± SEM. In some graphs, error bars were smaller than the symbol size and therefore not apparent. The best fit equation was determined visually and by using statistical criteria such as the residual sum of squared errors and an F-ratio test to determine whether adding additional parameters significantly improved the fit. Experiments were carried out at room temperature (20–22°C).

Solutions

The bath solution contained (in mM): NaCl 145; KCl 4; $CaCl_2$ 1.8; $MgCl_2$ 1.0; HEPES 10; and glucose 10, pH 7.35. The pipette solution contained

Received for publication 8 May 1995 and in final form 13 October 1995.

Address reprint requests to Paul B. Bennett, Ph.D., Department of Pharmacology, 560 MRB II, Vanderbilt University School of Medicine, Nashville, TN 37232-6602. Tel.: 615-936-1683; Fax: 615-322-4707.

0006-3495/96/01/238/08 $2.00

(intracellular solution) 10 mM NaF, 110 mM CsF, 20 mM CsCl, 10 mM EGTA, and 10 mM HEPES, pH 7.2.

Transfection of hH1 and hSkM1 cDNA for expression in tsA-201 cells

Transient transfection with calcium phosphate was used to express hSkM1 or hH1 in tsA-201 cells, which are a transformed human kidney cell line (HEK 293) stably expressing an SV40 T-antigen. Cell transfection was carried out using 10 μg of plasmid DNA encoding channel and 10 μg of salmon sperm DNA. These were placed in a microcentrifuge tube containing 0.5 mL of 250 mM calcium chloride. This solution was then added dropwise to a buffer solution and subsequently added onto cells in 100-mm dishes that were ~30% confluent. After ~24 h, the solution was changed to DMEM supplemented with 10% fetal bovine serum, 2 mM L-glutamine, penicillin (50 U/ml), and streptomycin (50 μg/ml), and cells were kept in a 37°C incubator until needed for patch clamping.

Expression constructs

A full-length hH1 coding sequence (nt. 151-6214) was constructed in the mammalian expression vector pRc/CMV (Invitrogen, San Diego, CA) by subcloning a 6.1-kb fragment from pSP64T-hH1 (Gellens et al., 1992) into the *Hind*III and *Xba*I sites of the vector. The 3′ *Sfi*I site of hH1 was made compatible with the vector *Xba*I site by using a 7-bp phosphorylated oligonucleotide adapter (5′-CTAGGCC-3′). Correct assembly of the final construct, designated pRc/CMV-hH1, was verified by restriction analysis and sequencing of the junctional regions. The pRc/CMV-hH1 construct contains the complete 5′-untranslated (UT) region of *Xenopus* β-globin from the pSP64T vector and only 15 bp of the native hH1 3′-UT. An earlier construct containing ~2.3 kb of the hH1 3′-UT expressed poorly. Construction of full-length pRc/CMV-hSkM1 has been described previously (Chahine et al., 1994).

RESULTS

Channel activation

Fig. 1 shows the voltage dependencies of channel gating for the cardiac (hH1) and skeletal muscle isoforms (hSkM1). In both cases, cells were held at a negative membrane potential (−120 mV) to remove inactivation, and steps were applied between −80 mV and +50 mV in 10-mV increments. The threshold and membrane potentials for half-maximal activation of the cardiac isoform were more negative than for the skeletal muscle isoform. Cardiac channels began to open at ~−60 mV. Fits of a Boltzmann function to the descending limb of the current-voltage relationship (see Fig. 1 legend) indicated that the cardiac channels were half maximally open at a membrane potential of −40 mV. In contrast, in the skeletal muscle isoform, the channels began opening at ~−45 mV and were half maximally open at a membrane potential of −25 mV. Peaks of the current voltage relationships (Fig. 1, *C* and *D*) were also different. The peak inward current occurred at ~−20 mV in the cardiac isoform, but occurred at −10 mV in the skeletal muscle isoform.

Rate of inactivation

A striking distinction between these two channel isoforms was the rate of decay of the current after channel opening (Hodgkin and Huxley, 1952a; Aldrich et al., 1983; Yue and Marban, 1989). To characterize the rate of macroscopic inactivation, we fitted the falling phase of the sodium current using exponential equations. Over most of the range of membrane potentials examined (−50 to +30 mV), hH1 required two exponentials to adequately describe the decay process. In contrast, hSkM1 was very well fit by a single exponential decay. The rate of inactivation of hSkM1 is significantly faster than the rate of inactivation of hH1 at membrane potentials >-10 mV ($p < 0.05$). Fig. 2 shows the time constants of inactivation as a function of membrane potential for the cardiac and skeletal muscle isoforms. The *open circles* indicate the time constants of fast inactivation for the skeletal muscle isoform. These range between ~1 ms at −30 mV and <0.2 ms at +40 mV. The *filled symbols* in Fig. 2 indicate the two time constants required for hH1. The fast time constant ranged between ~2 ms at −50 and

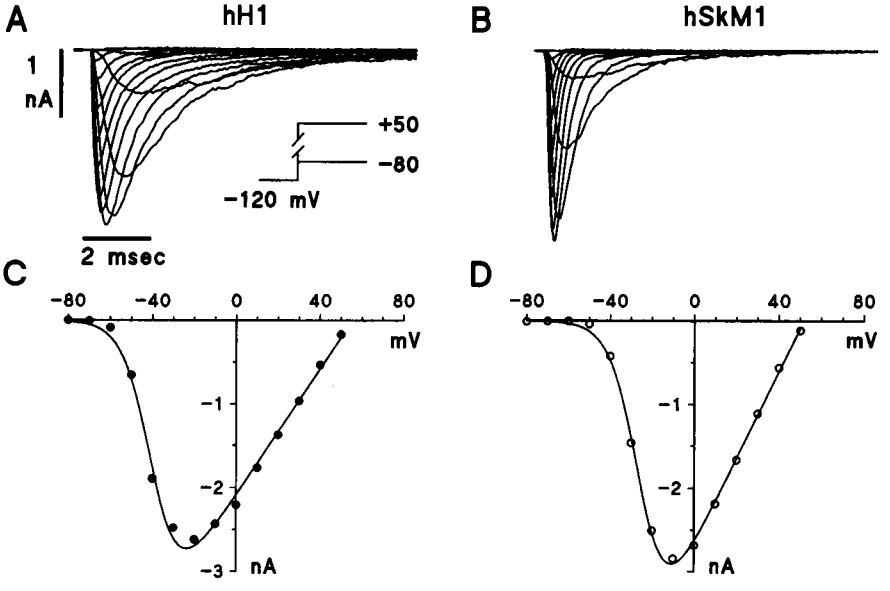

FIGURE 1 Current-voltage relationships for hH1 and hSkM1 in tsA-201 cells. (*A*) Raw current tracings for hH1 obtained at different voltage clamp step between −80 mV and +50 mV from holding potential of -120 mV. B. Raw current tracings obtained from hSkM1 tsA-201 cells using an identical pulse protocol. C. Peak inward current plotted as a function of membrane potential for hH1. D. Peak inward hSkM1 current plotted as a function of membrane potential. Solid curves through data points in C and D were generated by an equation containing the product of a Boltzmann function and a driving force term $I_{Na} = g_{Na} \cdot \{1 + \exp(V_m - V_{1/2})/k\}^{-1} \cdot \{V_m - E_{Na}\}$. The $V_{1/2}$ for the descending limb of the two curves were −40 and −25 mV for hH1 and hSkM1, respectively.

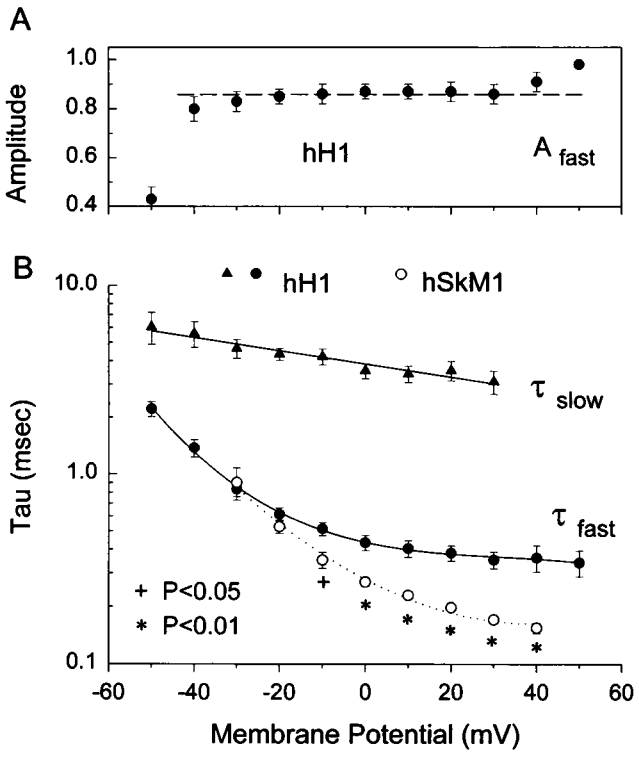

FIGURE 2 Voltage dependence of the rate of inactivation of hH1 and hSkM1. The falling phase of each record was fitted with an exponential function to obtain a quantitative estimate of the rate of inactivation. hH1 in general required a two-exponential function $y = A_1 \exp(-t/\tau_1) + A_2\exp(-t/\tau_2) + C$, whereas hSkM1 could be fitted with a single exponential function $y = A_1 \exp(-t/\tau_1) + C$. (*A*) The amplitude of the fast component (A_1) of hH1 inactivation is shown as a function of membrane potential. (*B*) Time constants of the falling phase of current for hH1 (n = 8) and hSkM1 (n = 9). hH1 was fitted with the sum of two exponential components. The means of these two time constants are shown as the solid symbols. hSkM1 could adequately be described with a single exponential function. The time constants for the rapid phase of decay for hH1 was significantly slower than that for hSkM1 at membrane potentials between −10 mV and +40 mV (+ $p < 0.05$; * $p < 0.01$).

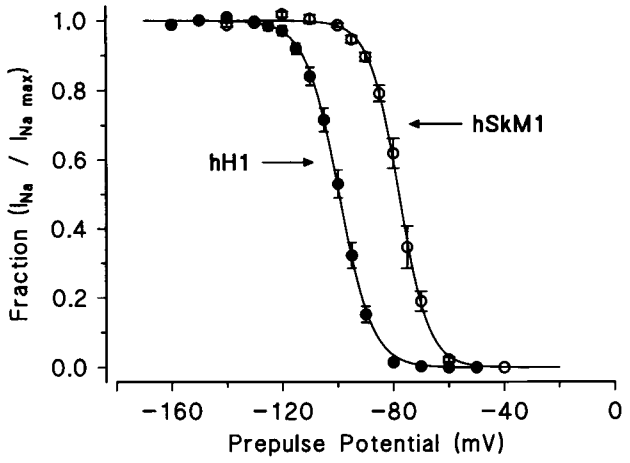

FIGURE 3 Voltage dependence of sodium channel availability. The voltage dependence of sodium channel availability for opening ("steady-state inactivation") was obtained using a standard double pulse protocol from a holding potential of −120 mV. The membrane potential was changed to the level displayed on the abscissa for a period of 500 ms. Subsequently the membrane potential was stepped to −20 mV to assay the available sodium current available. This was normalized to I by the current measured at −140 mV or −160 mV and used as an indication of the fraction of channels available to open after the 500 ms prepulse at the various membrane potentials. The solid curves represent nonlinear least-squares fits of the function $I/I\max = \{1 + \exp(V - V_{1/2})/k\}^{-1}$. Data for these experiments were obtained at 2–4 min after establishment of whole-cell dialysis for hSkM1 and hH1. The $V_{1/2}$ for hH1 was significantly more negative than that for hSkM1.

reached a limiting value of ~0.4 ms between −20 mV and +50 mV. The second slower process of inactivation was less potential-dependent, with time constants ranging between 6 and 3 ms over this range of membrane potentials. The relative amplitude of the fast component of hH1 is shown in the graphs above the time constants. Over most of the membrane potential range examined, this rapid component was ~85% of the total. Thus, in addition to the significant slow component in the cardiac isoform, the fast component of inactivation was significantly faster in the skeletal muscle isoform than the fast component of the cardiac isoform at membrane potentials ranging between −10 mV and +40 mV.

Steady-state inactivation

Fig. 3 characterizes the steady-state inactivation of these two isoforms using a standard two-pulse protocol with 500-ms prepulses. Individual and average data were fitted with a Boltzmann function (see Fig. 3 legend) to obtain the membrane potential of half-inactivation and the slope factor for the relationship. Under the conditions of our experiments, the cardiac isoform was half-inactivated at membrane potentials significantly more negative than those of the skeletal muscle isoform. The membrane potential for half-inactivation of hH1 was −99.6 ± 0.88 mV and the slope factor was 5.7 ± 0.33 mV, whereas the membrane potential for half-inactivation of the skeletal muscle isoform was −77.3 ± 1.03 mV, with a slope factor of 5.03 ± 0.24 mV. These differences in midpoint of the inactivation curve were statistically significantly different ($p < 0.001$; n = 11 and n = 9 for hH1 and hSkM1, respectively). The slope factors were not significantly different ($p > 0.1$).

Time-dependent changes in gating

Fig. 4 illustrates the time-dependent changes in the inactivation relationship in both the cardiac and the skeletal muscle isoforms. Curves shown in Fig. 4 *A* were obtained every 10 min during a continuous voltage-clamp recording. A similar experiment is shown for the skeletal muscle isoform in Fig. 4 *B*. In these experiments, we fitted Boltzmann relationships to these data and used the estimated membrane potential for half-maximal inactivation ($V_{1/2}$) to document the time-dependent shift of these availability relationships. Average data for the shift of the $V_{1/2}$ as a

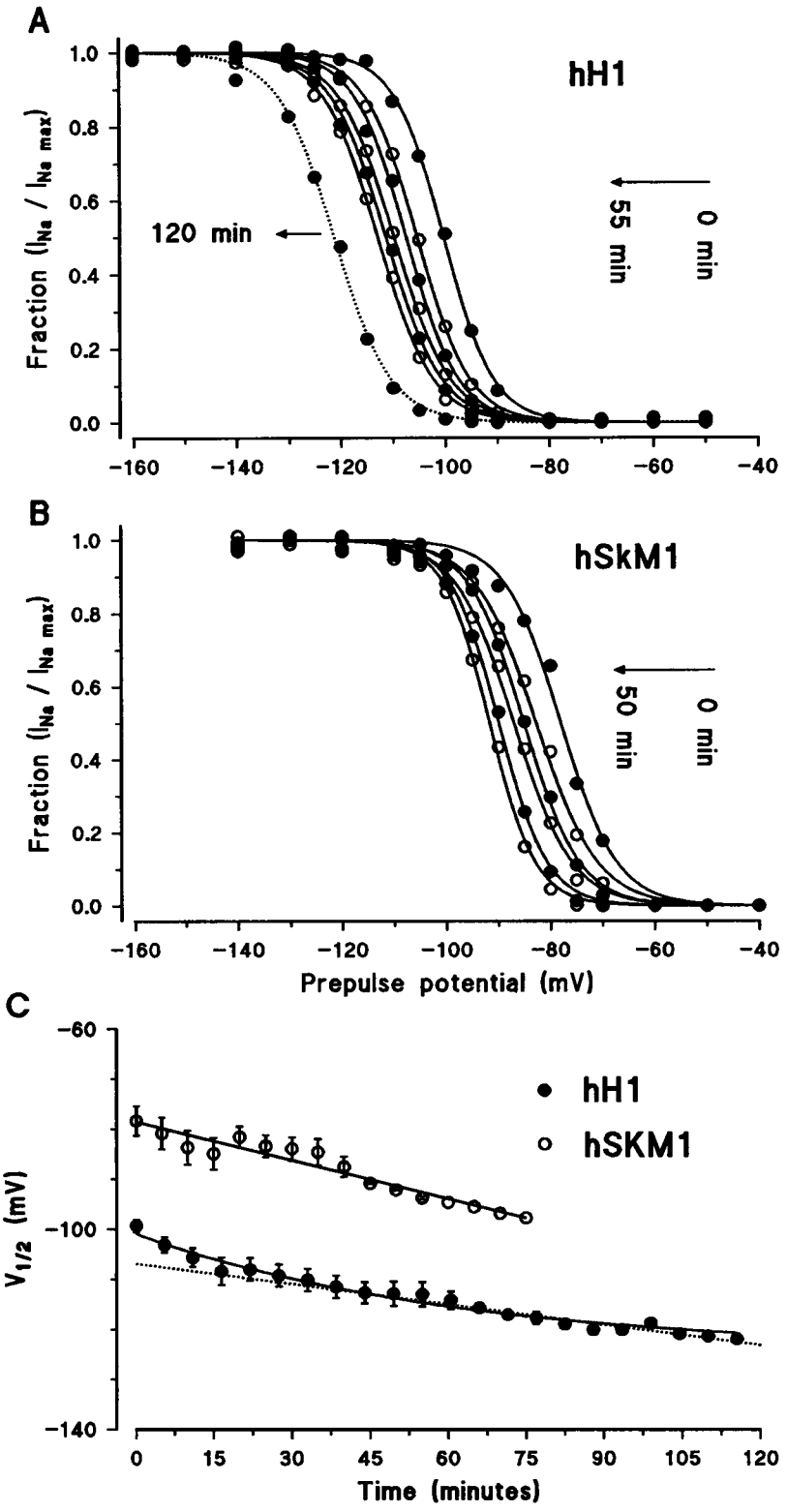

FIGURE 4 Shift of the availability relationships upon and after establishment of whole-cell dialysis for hH1 (*A*) and hSkM1 (*B*); time course of midpoint shift (*C*). Pulse protocols were identical to those used in Fig. 3 and were repeated every 10 min beginning within 5 min of establishment of whole-cell recording. Each curve was fitted with a Boltzmann function to estimate the voltage for half-maximal availability ($V_{1/2}$). The position of the availability relationship shifted as a function of time in the hyperpolarizing direction. Similar data were obtained in six to nine cells for both hH1 and hSkM1. There is a minimum uncertainty in the initial time value ($t = 0$) due to the time required for capacitance and series resistance compensation before recording. (*C*) After Boltzmann fitting of curves as shown, the $V_{1/2}$ data were averaged and plotted as a function of time after establishment of whole-cell recording. The symbols represent mean ± SEM for six to nine cells for hH1 and five to nine cells for hSkM1. The different numbers in the averages were determined by the durations of a given recording. The solid curve is a fitted exponential with a time constant of 63 min; the linear relationships have a slope of 0.135 mV/min for hH1 and 0.255 mV/min for hSkM1.

function of time during an experiment after formation of the gigaohm seal is shown for hH1 and hSkM1 in Fig. 4 *C*. The shift in the midpoint of the hH1 relationship is plotted as a function of time (*solid symbols*). The terminal linear shift is plotted as a *dotted line* and had a slope of 0.135 mV/min. Similar data for hSkM1 are plotted as *open symbols*. The best fit linear regression line is also shown with a slope of 0.255 mV/min.

Given the shifts in channel inactivation relationships, we wished to determine whether the voltage dependence for channel activation also changes with time. Fig. 5 shows current-voltage relationships for the cardiac isoform in Fig.

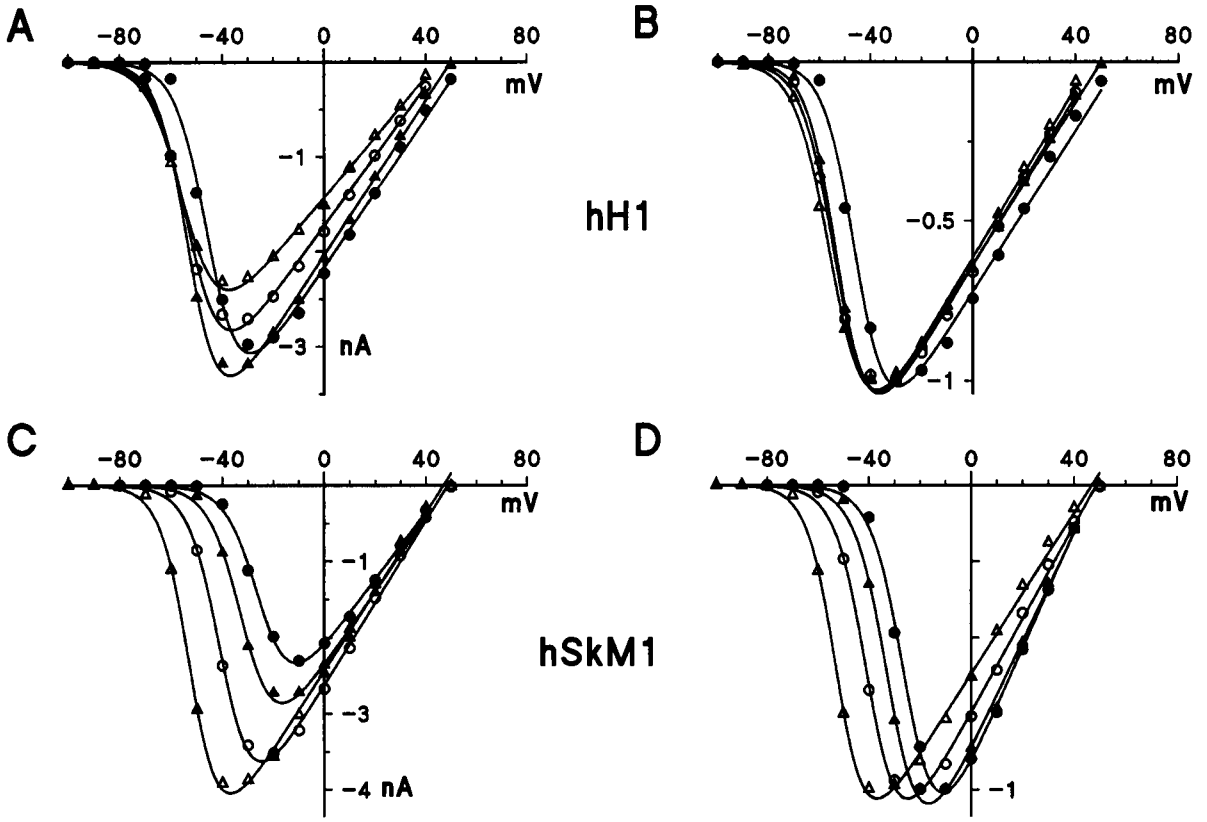

FIGURE 5 Current-voltage relationships for hH1 (*top*) and hSkM1 (*bottom*) obtained as a function of time after establishment of whole-cell recording. Data for each curve were obtained at 20-min intervals. (*A*) The raw data are shown; (*B*) the data were normalized to 1 to emphasize the position of the descending limb of the current-voltage relationship. Similar data are shown for hSkM1 in *C* and *D*. Note the larger degree of shift of the activation curve for hSkM1 compared with hH1. The filled circles indicate the initial measurement. Subsequent measurements were made at 20 (▲), 40 (○), and 60 min (△).

5, *A* and *B*, and for the skeletal muscle isoform in *C* and *D*. Current-voltage relationships were repeated at 20-min intervals after establishment of whole-cell dialysis. The descending limb of this current-voltage relationship is an indication of the activation range of the channel and the threshold for channel opening. Fig. 5 *A* presents data from the cardiac isoform (hH1) that show an initial small shift in the voltage dependence, which becomes relatively stable within 20 min. The magnitude of the hH1 current at the peak of the current-voltage relationship declines in this experiment because of the shift of the h_∞ curve, which results in fewer available channels at the holding potential. This confounding effect can be removed by normalizing the current, which is shown in Fig. 5 *B*. Here the relationship of the activation curves (*descending limb*) to one another as a function of time is more apparent. This behavior can be contrasted to that seen in the skeletal muscle isoform as shown in Fig. 5, *C* and *D*. In this case, the activation curve continued to shift with time to a greater extent than the inactivation voltage relationship, resulting in a shift of the midpoint of the descending limb of the current-voltage relationship and an increase in current due to the increased driving force at the more negative potentials. Fig. 5 *D* shows normalization of these data, again emphasizing the shift of the activation curve and that it was much greater than the shift of the cardiac isoform. In addition, the shift continued over the time period shown. Similar data were obtained in four additional cells for hH1 and in five cells for hSkM1.

Fig. 6 illustrates the effect of ~1 h of whole-cell recording on the sodium channel kinetics measured at −20 mV. Little or no change was observed in hH1; however, hSkM1 kinetics were markedly changed. The time to peak current occurred earlier, and the inactivation rate was faster after 50 min of recording. These differences in hH1 and hSkM1 suggest that the mechanism causing the shift in kinetics of activation is distinct from the mechanism that causes the inactivation kinetic shift.

We also made measurements of recovery from inactivation within the first 5 min of establishment of whole-cell dialysis. Recovery from inactivation was fitted by a double exponential equation, as indicated in the legend to Fig. 7. As seen in Fig. 7, in general the cardiac isoform recovered more slowly than did the skeletal muscle isoform. The figure show the averaged time course of recovery, and the *inset* shows the best fit parameters to this average. We also fitted the curves from each experiment individually with similar results. Both isoforms had a rapid component of recovery that occurred with time constants of 2.1 ± 0.4 ms

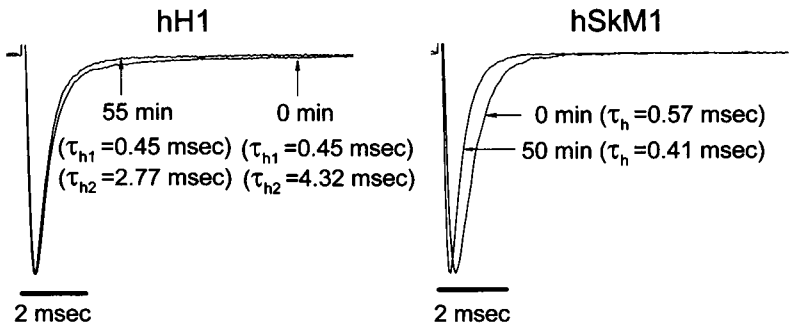

FIGURE 6 Time dependence of hH1 and hSkM1 current kinetics at −20 mV. (*Left*) hH1 current was measured from a holding potential of −120 mV during a step to −20 mV. Two recordings are shown 55 min apart. The first recording was taken upon initially breaking into the cell, and the second was taken 55 min later. Similar tracings (*right*) for an hSkM1 transfected cell taken 50 min apart. There is little or no change in the kinetics of activation or inactivation for hH1. hSkM1 activates faster, peaks sooner, and inactivates somewhat faster after 50 min of whole-cell dialysis.

(n = 7) for hSkM1 and 7.5 ± 0.7 ms (n = 13) for hH1. The amplitude of this component was 76.9 ± 5.6% for hSkM1 and 79.7 ± 7.6% for hH1. Both isoforms also had a slower component of recovery with amplitudes of 23.1 ± 5.1% and 20.3 ± 4.3% and time constants of 56.0 ± 9.3 ms and 40.9 ± 5.2 ms for hH1 and hSkM1, respectively. Although in general hH1 recovered more slowly from inactivation, these data indicate that both channels had fully recovered within 200 ms.

DISCUSSION

In this study we expressed the recombinant human cardiac sodium channel (hH1) expressed in a mammalian cell line and compared its gating to the human skeletal muscle isoform (hSkM1). Both the brain and the skeletal muscle sodium channel isoforms display abnormal kinetic characteristics when expressed in *Xenopus* oocytes (Krafte et al., 1990; Zhou et al., 1991). This deficit can be corrected by coexpression with a β_1 subunit (Isom et al., 1992; Bennett et al., 1993), although the mechanism of this effect is not fully known. Unlike expression in oocytes in which hSkM1 gating is anomalously slow compared with hH1, in general hSkM1 gating was faster than that of hH1 when expressed in mammalian cells. The rates of activation and recovery from inactivation were all greater in hSkM1 compared with hH1. In the absence of precise structural information on ion channel proteins, a current strategy is to use site-directed mutagenesis or to generate chimeric channels to try and determine the structural basis for functional differences. To achieve these goals, it is necessary to define functional distinctions among ion channel isoforms. It is with this background that the present study was undertaken. In addition, if future studies are to involve characterization of drugs or gating of either the human cardiac or the human skeletal isoform, it is essential to determine how these channels behave in a heterologous expression system. Our experiments were designed to express these distinct channels in identical cells under identical conditions using similar voltage-clamp protocols to best characterize their similarities and differences.

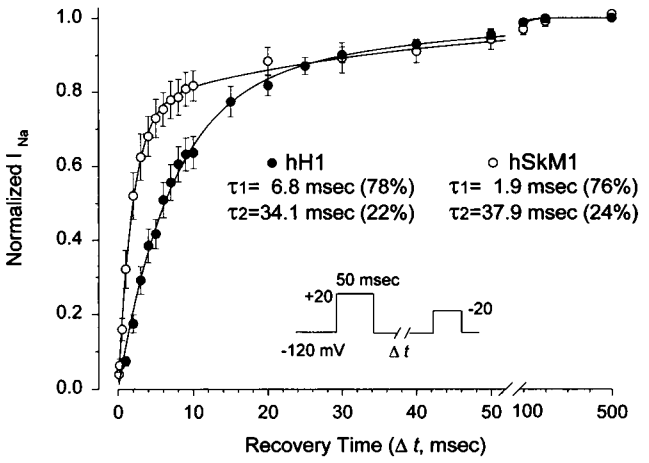

FIGURE 7 Time course of recovery from inactivation at −120 mV. The pulse protocol for measuring recovery from inactivation is shown as an inset. The holding potential was −120 mV; a prepulse to +20 mV was applied for 50 ms, and the membrane potential was changed back to −120 mV for the period of time indicated on the abscissa. A test pulse to −20 mV was then applied to access the fractional recovery of current after complete inactivation during the prepulse. The currents were normalized by the maximum current at −20 mV obtained after a 10-s interval at −120 mV. The time course of this recovery is shown and was fitted with a double exponential function curve for hH1 (*open symbols*) and hSkM1 (*filled symbols*): $I(t)/I_{max} = 1 - \{A_1 e^{-t/\tau 1} + A_2 e^{-t/\tau 2}\}$. The means of 8–12 cells are shown for hH1 and of 7–8 cells for hSkM1. The best fit parameters (τ_1, τ_2, A_1, A_2) obtained from fitting the averaged data are shown as an inset. The averaged parameters obtained from fitting individual recoveries are provided in the text. Almost all current is recovered in both types of channel by 100 ms, and complete recovery had occurred by 200 ms. At shorter intervals, hH1 recovered significantly less than did hSkM1. These data were obtained 2–5 min after initial whole-cell dialysis.

Chahine et al. (1994) previously provided a partial characterization of the human skeletal muscle sodium channel in *Xenopus* oocytes and tsA-201 cells. It was shown that the human skeletal muscle isoform is sensitive to tetrodotoxin with an IC_{50} of 25 ± 2.4 nM. The time constants for inactivation when expressed in tsA-201 cells ranged between 3.5 ms at −30 mV and 0.4 ms at +30 mV. The single-channel conductance in outside-out patches was 24.9 pS in oocytes. The voltage dependence of steady-steady inactivation was not characterized nor was the time course for recovery from inactivation characterized.

A recent study of cardiac sodium channels in human atrial myocytes obtained from biopsies was reported by Schneider et al. (1994). The threshold for sodium current activation was −64 mV. The time constant of inactivation was 2 ms at −55 mV and asymptotically approached 0.2 ms at positive membrane potentials. The steady-state inactivation with a 512-ms prepulse indicated a voltage for half-

maximal inactivation of −72.2 mV, with a slope factor of 4.9 mV. The time constants of recovery from inactivation at −125 mV were 4.7 and 19.8 ms and at −95 mV were 15.9 and 53.2 ms. These data are similar to our own data for the human recombinant α subunit expressed in tsA-201 cells. The main difference seemed to be in the midpoint of the steady-state (500 ms) inactivation curve, which in our experiments was more negative than that reported by Schneider et al. (1994). This difference can be accounted for at least in part by the nonstationary position of this curve in both of our experiments.

Both the cardiac and the skeletal muscle isoforms displayed time-dependent shifts of gating kinetic parameters, as has been described previously for Na^+ current in whole-cell recordings in other cells. This behavior has been noted previously in native cells (Sheets and Hanck, 1993; Gonoi and Hille, 1987; Fenwick et al., 1982), although Gonoi and Hille (1987) demonstrated that such a shift did not occur in N18 cells but did occur in GH_3 cells. These time-dependent changes in gating are potential confounding variables for studies of channel mutants or drugs in these cells. Therefore, we wished to determine whether this problem occurred with either of these isoforms when transfected into tsA-201 cells. The midpoint of the channel availability curve for cardiac isoform was initially more negative than the skeletal muscle channel and shifted in the negative direction more slowly. The channel activation voltage relationship also shifted markedly with time for hSkM1 but much less so with hH1. The combined negative shifts of the "activation" and "inactivation" relationships and their distinct rates of shift caused differences in the appearance of hH1 and hSkM1 currents over time. From very negative holding potentials (−120 mV), hH1 current was stable or declined, whereas hSkM1 current increased with time. This difference in behavior can be attributed to the relatively greater leftward shift of the activation curve compared with the inactivation curve in hSkM1.

In Fig. 5, the voltage dependence of channel activation seems to shift slightly and then saturate for hH1, whereas it continues to shift for hSkM1. These shifts occur in conjunction with the shifts in the sodium channel availability relationships as shown in Fig. 4. A Hodgkin and Huxley (1952b) type model, in which the rate constants for opening and closing determine the steady-state positions of the activation and inactivation curves, predicts that for a given shift in either activation or inactivation curves there should also be a change in the kinetics of the channel. Fig. 6 (*left*) shows raw current tracings from the same experiment as shown in Fig. 4 for hH1. These raw currents, obtained 55 min apart, have essentially identical kinetics. There was a very slight change in inactivation (Fig. 6, *left*) after 55 min for hH1 because of a decrease in the minor slow time constant. In contrast, the kinetic changes of hSkM1 (Fig. 6, *right*) were much more apparent. After 50 min of whole-cell dialysis, the currents activated faster, and the peak current occurred earlier and inactivation was faster. These observations indicate that the shifts in the activation and inactivation curves are dissociated from one another in the two channel types; the process causing the shift in the inactivation curve of hH1 is not a change in the rate constants that determine the time course of the sodium current for this channel. This is not the case for steady-state inactivation of hSkM1. Both the activation and the inactivation relationship shift with time, and the kinetics change as well.

These results have implications both for drug studies using these channels and for interpretation of mutant channels expressed in heterologous systems. An active area of research involves the placement of mutations observed in disease into wild-type channels to observe the functional consequences. Our data indicate that care should be taken when interpreting apparent kinetic and voltage-dependent changes because the observed effects could be caused by the phenomena that we have described and not by the mutations per se. Similar precautions must be taken in drug studies because a control measurement may not be compared appropriately to a drug effect if they are recorded too far apart in time.

This work was supported by grants HL51197 and HL46681 (Paul B. Bennett) from the National Institutes of Health. Alfred George, Jr., is a Lucille P. Markey Scholar. Paul B. Bennett is an Established Investigator of the American Heart Association.

REFERENCES

Aldrich, R. W., D. P. Corey, and C. F. Stevens. 1983. A reinterpretation of mammalian sodium channel gating based on single channel recording. *Nature (Lond.).* 306:436–441.

Armstrong, C. M. Sodium channels, and gating currents. 1981. *Physiol. Rev.* 61:644–682.

Bennett, P. B., N. Makita, and A. L. George, Jr. 1993. A molecular basis for gating mode transitions in human skeletal muscle Na^+ channels. *FEBS Lett.* 326:21–24.

Catterall, W. A. 1992. Cellular and molecular biology of voltage-gated sodium channels. *Physiol. Rev.* 72:15–48.

Chahine, M., P. B. Bennett, A. L. George, Jr., and R. Horn. 1994. Functional expression and properties of the human skeletal muscle sodium channel. *Pflugers Arch.* 427:136–142.

Fenwick, E. M., A. Marty, and E. Neher. 1982. Sodium and calcium channels in bovine chromaffin cells. *J. Physiol. (Lond.).* 331:599–635.

Gellens, M. E., A. L. George, Jr., L. Chen, M. Chahine, R. Horn, R. L. Barchi, and R. G. Kallen. 1992. Primary structure and functional expression of the human cardiac tetrodotoxin-insensitive voltage dependent sodium channel. *Proc. Natl. Acad. Sci. USA.* 89:554–558.

George, A. L., J. Komisarof, R. G. Kallen, and R. L. Barchi. 1992. Primary structure of the adult human skeletal muscle voltage-dependent sodium channel. *Ann. Neurol.* 31:131–137.

Gonoi, T., and B. Hille. 1987. Gating of Na channels. Inactivation modifiers discriminate among models. *J. Gen. Physiol.* 89:253–274.

Hille, Bertil. 1992. Ionic Channels of Excitable Membranes, 2nd ed. Sinauer Associates, Sunderland, MA.

Hodgkin, A. L., and A. F. Huxley. 1952a. Currents carried by sodium and potassium ions through the membrane of the giant axon of *Loligo. J. Physiol. (Lond.).* 116:449–472.

Hodgkin, A. L., and A. F. Huxley. 1952b. A quantitative description of membrane current and the application in conduction and excitation of nerve. *J. Physiol. (Lond.).* 117:500–544.

Isom, L. L., K. S. De Jongh, D. E. Patton, B. F. X. Reber, J. Offord, H. Charbonneau, K. Walsh, A. L. Goldin, and W. A. Catterall. 1992.

Primary structure and functional expression of the β_1 subunit of the rat brain sodium channel. *Science.* 256:839–842.

Krafte, D. S., A. L. Goldin, V. J. Auld, R. J. Dunn, N. Davidson, and H. A. Lester. 1990. Inactivation of cloned Na channels expressed in *Xenopus* oocytes. *J. Gen. Physiol.* 96:689–706.

Noda M., T. Ikeda, T. Kayano, H. Suzuki, H. Takeshima, M. Kurasaki, H. Takahashi, and S. Numa. 1986a. Existence of distinct sodium channel messenger RNAs in rat brain. *Nature (Lond.).* 320:188–192.

Noda M., T. Ikeda, T. Kayano, H. Suzuki, H. Takeshima, M. Kurasaki, H. Takahashi, M. Kuno, and S. Numa. 1986b. Expression of functional sodium channels from cloned cDNA. *Nature (Lond.).* 322:826–828.

Rogart, R. B., L. L. Cribbs, L. K. Muglia, D. D. Kephart, and M. W. Kaiser. 1989. Molecular cloning of a putative tetrodotoxin-resistant rat heart sodium channel isoform. *Proc. Natl. Acad. Sci. USA.* 86:8170–8174.

Schneider, M., T. Proebstle, V. Hannekum, and R. Rudel. 1994. Characterization of the sodium currents in isolated human cardiocytes. *Pflugers Arch.* 428:84–90.

Sheets, M. F., and D. A. Hanck. 1993. Modification of sodium channel inactivation by α-chymotrypsin in canine cardiac Purkinje cells. *J. Cardiovasc. Electrophysiol.* 4:686–694.

Trimmer, J. S., S. S. Cooperman, S. A. Tomiko, J. Y. Zhou, S. M. Crean, M. B. Boyle, R. G. Kallen, Z. H. Sheng, R. L. Barchi, F. J. Sigworth, R. H. Goodman, W. S. Agnew, and G. Mandel. 1989. Primary structure and functional expression of a mammalian skeletal muscle sodium channel. *Neuron.* 3:33–49.

Valenzuela, C., and P. B. Bennett. 1994. Gating of Na^+ channels in excised membrane patches after modification by α-chymotrypsin. *Biophys. J.* 67:161–171.

Yue, D. T., J. H. Lawrence, and E. Marban. 1989. Two molecular transitions influence cardiac sodium channel gating. *Science.* 244:349–352.

Zhou J., J. F. Potts, J. S. Trimmer, W. S. Agnew, F. J. Sigworth. 1991. Multiple gating models and the effect of modulating factors on the μI sodium channel. *Neuron.* 7:775–785.